Diagn Interv Radiol 2006; 12:115-120

Evaluation of parenchymal changes at the operation site with early postoperative brain diffusion-weighted magnetic resonance imaging

Arzu Öztürk, Kader Karlı Oğuz, Nejat Akalan, Pınar Özdemir Geyik, Ayşenur Cila

PURPOSE
To evaluate diffusion changes in the brain parenchyma at the operation site during the first 24 hours following surgery.

MATERIALS AND METHODS
The study group consisted of 52 patients, 39 who had tumor resection surgery and 13 who had epilepsy surgery. Early postoperative magnetic resonance imaging (MRI) included diffusion-weighted imaging (DWI) and routine contrast-enhanced cranial MRI, together with T2* weighted images on a 3T system. DWI findings and the presence of hemorrhage in the brain parenchyma were evaluated. Correlation between the findings, the primary lesion leading to surgery, and operation site were evaluated.

RESULTS
Diffusion restriction in the parenchyma surrounding the resection cavity was seen in 17 tumor patients (32.7%, n = 52) and in 8 epilepsy patients (15.4%, n = 52). DWI showed increased diffusion in 7 patients and no abnormality in 4 patients. Twenty patients showed restricted diffusion pattern related to hemorrhage (38.5%, n = 52).

CONCLUSION
Restricted diffusion was the most common abnormality observed in the early postoperative DWI of brain parenchyma at the operation site after surgery, which suggested tissue injury caused by surgery. Yet, hemorrhaging in the operation bed can constitute another cause of a reduced apparent diffusion coefficient (ADC) value. Increased diffusion and normal diffusion can also be observed, though rarely.

Key words: • *brain* • *postoperative* • *diffusion weighted MRI*

From the Departments of Radiology (A.Ö. ✉ *karlioguz@yahoo.com*, K.K.O., A.C.), Neurosurgery (N.A.), and Biostatistics (P.Ö.G.), Hacettepe University, School of Medicine, Ankara, Turkey.

Received 20 February 2006; revision requested 10 April 2006; revision received 31 July 2006; accepted 1 August 2006.

Magnetic resonance imaging (MRI) has been typically performed within 48 h of brain surgery in many centers to evaluate immediate post-procedural changes. Postoperative neuroimaging findings provide a guide for further therapies and follow-up imaging. Diffusion-weighted imaging (DWI), as a part of routine brain MRI examinations, can be a useful tool in the evaluation of immediate post-procedural changes (1, 2).

Our review of several clinical cases has suggested that foci of diffusion restriction may appear in many recently operated patients. A recent study has also documented abnormal findings on DWI following surgery for infiltrating gliomas (2). We aimed to determine the frequency and evolution of such tissue changes in follow-up imaging, as well as any correlations between the findings and pre-operative tumor size, tumor histopathology, the presence of residual tumors in cases with tumor resection, the location of the surgery, and presence of hemorrhages in the operation beds in all cases. The initial examinations were performed within the first postoperative 24 h and diffusion patterns were compared to the normal contralateral parenchyma.

Materials and methods

The study group consisted of 52 patients (23 female, 29 male; age range: 8 months-80 years: mean age: 27 years) who had undergone intracranial surgery. Patients who had an unexpected immediate postoperative clinical course were excluded from the study. Indications for surgery were an intracranial tumor in 39 patients and mesial temporal sclerosis (MTS) and/or cortical dysplasia in 13 patients. MRI was performed in all patients within the first 24 h following surgery and included routine contrast-enhanced cranial MRI and single-shot gradient-echo (GRE) echo planar DWI (TR/TE: 2800/78 msec; matrix: 256x256; b value: 0, 500, and 1000 s/mm^2 diffusion gradients applied along 3 orthogonal planes) on a 3T MR system equipped with gradients at 33mT/m strength and 160 ms/mT slew rate (Allegra, Siemens, Erlangen, Germany). All axial images were acquired with a 5 mm slice thickness and 10% interslice gap. A total of 20 slices, which enabled whole-brain coverage were obtained. Twenty tumor patients also underwent T2* GRE imaging and 24 had additional computed tomography (CT) (5 patients with tumors had both) during the same session as DWI. In total, 29 patients underwent T2* GRE imaging and 28 had computed tomography (CT). Fifteen patients had repetitive DWIs between the 7th postoperative day and one month.

Diffusion changes in brain parenchyma were evaluated by 3 radiologists in consensus, who visually compared the signal intensity of lesions with that of normal parenchyma of the contralateral hemisphere on the same slice of DWI. The apparent diffusion coefficient (ADC) values were also measured from the parenchyma near the operation site and

Table.

Patient No.	Sex/Age	Primary lesion	Surgery location	ADC values of surgery site ($\times 10^{-3}$ s/mm^2)	ADC values of contralateral normal appearing parenchyma ($\times 10^{-3}$ s/mm^2)	Blood-related diffusion abnormalities
1	F/37 yr	Oligodendroglioma	S	0.45	1	-
2	M/34 yr	Oligodendroglioma	S	0.59	0.93	-
3	F/38 yr	Anaplastic oligoastrocytoma	I	0.50	0.90	-
4	F/45 yr	Anaplastic oligoastrocytoma	S	0.65	0.96	+
5	M/3 yr	Pilocytic astrocytoma	I	0.70	0.95	+
6	M/2 yr	Pilocytic astrocytoma	S	1.18	0.87	-
7	M/6 yr	Astroblastoma	S	0.54	0.95	+
8	F/17 yr	Mixed glial	I	0.66	0.93	-
9	M/35 yr	Glioblastoma	S	1.27	0.82	+
10	M/32 yr	Glioblastoma	S	0.45	0.85	-
11	F/56 yr	Glioblastoma	S	1.54	0.78	-
12	M/ 8 mo	Ganglioglioma	S	0.46	1.04	-
13	M/5 yr	Ganglioglioma	S	0.61	0.85	+
14	M/11 yr	Anaplastic ependymoma	S	0.63	1.12	+
15	M/13 yr	Anaplastic ependymoma	S	0.61	0.86	+
16	M/2 yr	Anaplastic ependymoma	I	1.23	0.87	+
17	F/6 yr	PNET	S	0.51	0.86	+
18	F/9 yr	PNET	S	0.59	0.99	-
19	M/29 yr	DNET	S	0.49	0.88	+
20	M/9 yr	DNET	S	0.47	0.86	+
21	M/24 yr	DNET	S	0.66	0.82	-
22	M/12 yr	Medulloblastoma	I	0.87	0.95	+
23	M/16 yr	Medulloblastoma	I	0.64	0.86	-
24	F/7 yr	Medulloblastoma	I	0.80	0.82	-
25	M/4 yr	Medulloblastoma	I	0.60	0.85	-
26	M/5 yr	Medulloblastoma	I	0.53	0.88	-
27	F/29 yr	Hemangioblastoma	I	0,89	0.76	-
28	M/30 yr	Hemangioblastoma	I	0.53	0.96	-
29	M/18 yr	Hemangioblastoma	I	0.46	0.79	+
30	F/53 yr	Metastasis	I	1.37	0.79	-
31	M/80 yr	Meningioma	S	0.45	0.80	+
32	F/79 yr	Meningioma	S	0.70	1.1	+
33	F/34 yr	Meningioma	S	0.59	0.84	-
34	F/42 yr	Meningioma	S	0.62	0.90	-
35	M/46 yr	Meningioma	I	1.00	0.81	-
36	F/44 yr	Meningioma	S	0.55	0.73	-
37	F/61 yr	Craniopharyngioma	S	0.52	0.84	-
38	M/72 yr	Craniopharyngioma	S	0.60	0.80	+
39	F/37 yr	Pineocytoma	S	0.51	0.76	-
40	M/49 yr	Cortical dysplasia	S	0.51	0.74	+
41	F/12 yr	Cortical dysplasia	S	0.66	1.09	+
42	M/14 yr	Cortical dysplasia	S	0.55	0.96	-
43	M/11 yr	Corpus callosotomy	S	0.50	0.86	-
44	M/16 yr	MTS	S	0.41	0.88	-
45	M/23 yr	MTS	S	0.55	0.96	-
46	F/51 yr	MTS	S	0.63	0.79	-
47	F/25 yr	MTS	S	0.85	0.80	-
48	M/39 yr	MTS	S	0.50	0.88	+
49	F/32 yr	MTS	S	0.66	0.90	-
50	F/27 yr	MTS	S	0.54	0.91	-
51	F/34 yr	MTS	S	0.44	0.89	-
52	F/24 yr	MTS	S	1.12	0.89	+

M = male; F = female; PNET = primitive neuroectodermal tumor; DNET = dysembryoplastic neuroepithelial tumor; MTS = mesial temporal sclerosis; S = supratentorial; I = infratentorial; yr = years; mo = months

from contralateral normal-appearing brain parenchyma by one radiologist (AO). Each region of interest (ROI) was placed manually on calculated average ADC maps if abnormal signal intensity was noted as focal areas adjacent to the resection cavity by using the largest ROI possible within the area. In the case of a thin, linear rim of diffusion abnormality around the surgery site, ROI was selected as a pixel. Each ROI was mirrored on to the normal appearing contralateral hemisphere in all patients. The selection of ROIs was made adjacent to the resection sites, excluding cerebrospinal fluid spaces. In our study group, there was no surgical material left in the surgical cavity after the completion of the surgical procedures. To avoid errors in ROI selection, patients with surgery-related changes, i.e., air in the ventricles, subarachnoid space, or resection cavity, and surgical sutures that caused distortion, were excluded. Any hemorrhagic changes in brain parenchyma that would have interfered with true parenchymal diffusion change were noted by CT and/or GRE imaging. In patients who did not have CT or T2* GRE, to evaluate hemorrhagic changes near the resection site, one radiologist (AO) retrospectively reviewed images generated from the diffusion sequence with diffusion sensitivity b = 0. In the cases with an intracranial tumor, any effects on diffusion abnormalities by pre-operative tumor size, tumor pathology, and presence of a residual tumor following surgery were also explored. Statistical analysis was performed with t test and chi-square test; $p < 0.05$ was accepted as significant in all tests.

Results

Twenty-five of the tumors were supratentorial and 14 were infratentorial. The operation sites of the subjects who underwent cranial surgery because of non-tumoral etiology were supratentorial. Results of histopathological examination of all the tumors and etiologies for non-tumoral surgery are shown in Table. We found restricted diffusion in the parenchyma adjacent to the resection cavity in 17 patients (32.7%) who had tumor surgery and in 8 patients (15.4%) who had epilepsy surgery (Figures 1-3). The ADC maps of 7 patients (13.4%) showed abnormalities suggesting increased diffusion. No diffusion abnormality was observed in 4

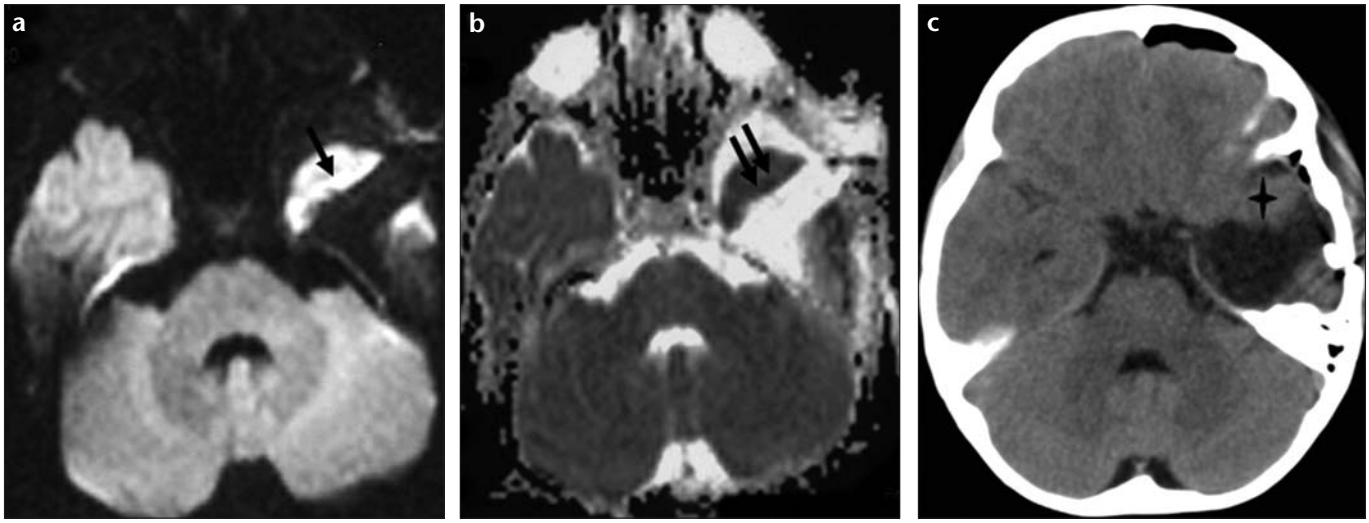

Figure 1. a-c. Case 18. A 9-year-old female. Early postoperative transverse diffusion-weighted (DWI) and computed tomographic (CT) images of a primitive neuroectodermal tumor (PNET). Transverse DWI **(a)** with corresponding ADC (apparent diffusion coefficient) map **(b)**, which indicates restricted diffusion *(single arrow in* **a** *and double arrows in* **b***)* around the resection cavity. There was no blood around the cavity *(asterisk)* as shown on transverse CT scan **(c)**.

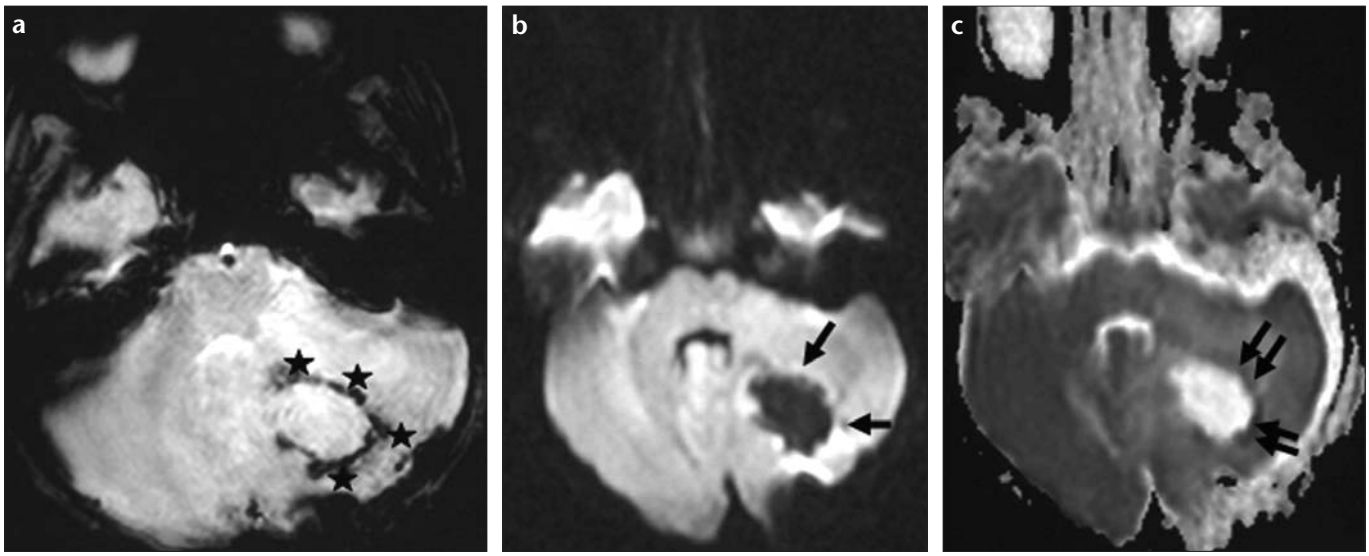

Figure 2. a-c. Case 5. A 3-year-old male. Early postoperative transverse T2* weighted image **(a)** diffusion-weighted image (DWI) **(b)**, and ADC (apparent diffusion coefficient) map **(c)** of a pilocytic astrocytoma. Mixed deoxy- and methemoglobin encircling the resection cavity *(stars)* is seen on transverse T2*GRE image **(a)**. Thus, restricted diffusion with high intensity on DWI *(individual arrows,* **b***)* and low value on ADC map *(double arrows,* **c***)* is the result of hemorrhage.

cases (7.6%). Twenty patients (38.4%) had signal abnormalities related only to hemorrhages, which mostly showed restricted diffusion (Figure 2), whereas 3 patients had increased ADC and one patient had no diffusion abnormality.

Based on these data, the most common DWI finding around the resection cavity during the early postoperative period was restricted diffusion. Reversal of high signal on DWI was observed in every case that had follow-up imaging (Figure 3); however, there was a correlation between diffusion abnormalities and surgery site; i.e., a restricted diffusion pattern was more common in those patients that had a supratentorial surgical approach ($p < 0.05$, Fisher's Chi-Square test). Statistical analysis revealed no correlation between diffusion changes and pre-operative tumor size, histopathology, and the presence of a residual tumor ($p > 0.05$, Fisher's Chi-Square test).

Discussion

Pathological processes disturb the texture of tissue either by destruction, degeneration of membranous elements, or by changes in cellularity and/or water content of tissue compartments. Alterations in permeability, osmolarity, or active transportation may cause shifts in the amount of the water protons in tissue compartments, which can be observed with DWI (3, 4). Based on different diffusion characteristics of cytotoxic and other types of tissue edema, DWI has been used for the evaluation of cerebral ischemia, edema, differentiation of necrotic-cystic tumors vs. abscesses and non-enhanced tumor infiltration vs. vasogenic edema, and de/dysmyelination (5-10).

A recent report states that the occurrence of restricted diffusion in and around the resection site immediately after brain tumor resection surgery is

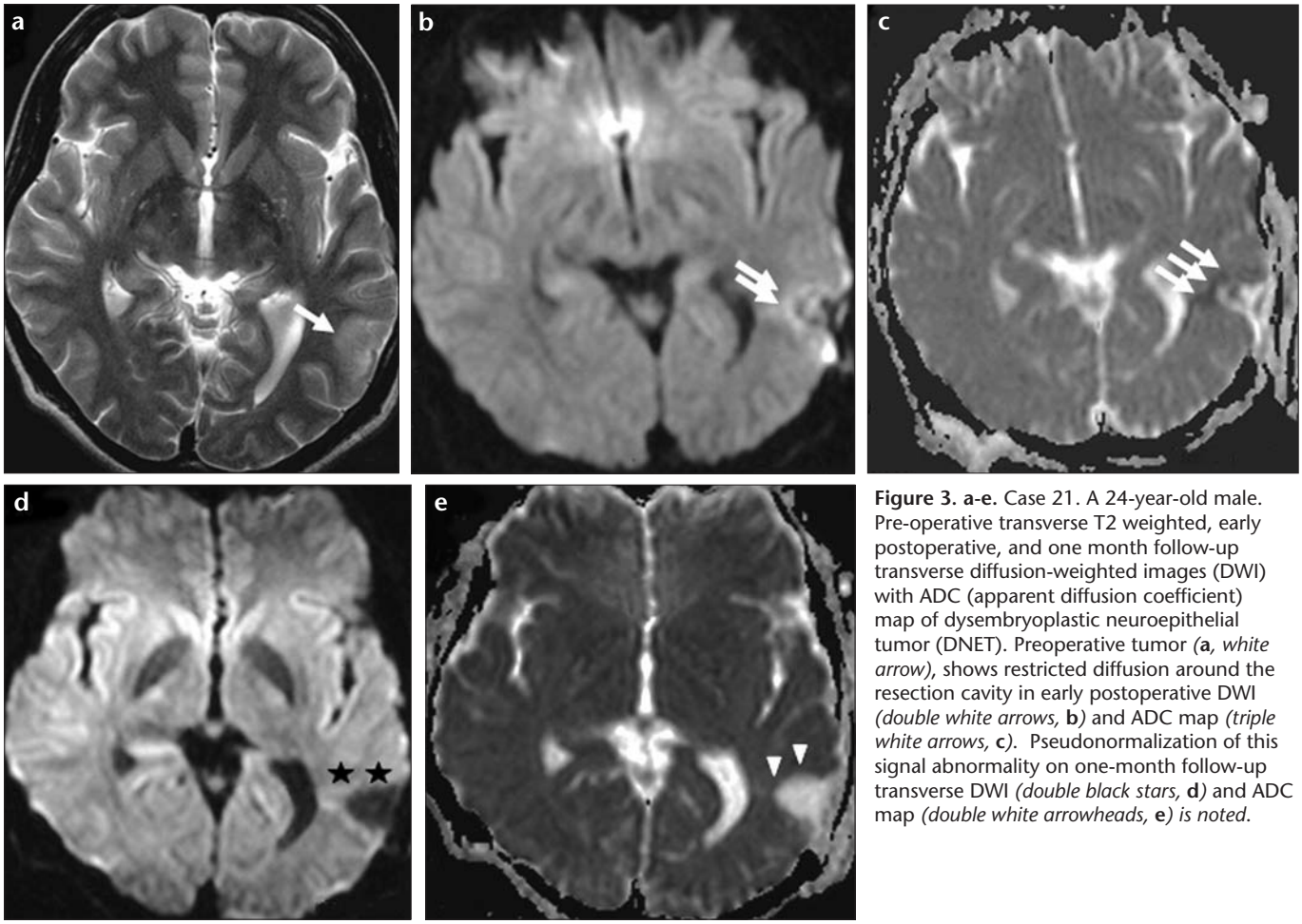

Figure 3. a-e. Case 21. A 24-year-old male. Pre-operative transverse T2 weighted, early postoperative, and one month follow-up transverse diffusion-weighted images (DWI) with ADC (apparent diffusion coefficient) map of dysembryoplastic neuroepithelial tumor (DNET). Preoperative tumor *(**a**, white arrow)*, shows restricted diffusion around the resection cavity in early postoperative DWI *(double white arrows, **b**)* and ADC map *(triple white arrows, **c**)*. Pseudonormalization of this signal abnormality on one-month follow-up transverse DWI *(double black stars, **d**)* and ADC map *(double white arrowheads, **e**) is noted*.

not uncommon (2). In that study, the authors observed a restricted diffusion pattern in 64% of patients and found complete resolution in 86% within 90 days. Diffusion abnormalities typically resolved, were replaced by contrast enhancement on follow-up imaging, and demonstrated encephalomalacia on long-term follow-up imaging. Similar to the evolution of restricted diffusion in acute infarct areas, immediate postoperative diffusion abnormalities invariably undergo a phase of contrast enhancement on routine images that can be easily misinterpreted as tumor recurrence. This study also found that regions of restricted diffusion after glioma surgery showed contrast enhancement on follow-up MRI, simulating the appearance of recurrent tumor. These areas of enhancement invariably evolved into encephalomalacias or gliotic cavities in long-term follow-up studies, as one would expect in a region of permanent brain injury (2).

Our study was not planned to investigate diffusion changes caused by recurrent or residual tumors around the resection cavity, but rather tumor or epilepsy surgery-related diffusion changes. We observed that restricted diffusion patterns were the most common (48.1%) early DWI abnormality in the resection site.

A widely accepted theory for the restriction of water diffusion in tissues relies on the disruption of energy metabolism, a decline in cellular adenosine triphosphate (ATP), and failure of the Na^+/K^+ and Ca^{2+} membrane pumps with resultant cellular retention of water, known as 'cytotoxic edema' (11, 12). Additionally, increased tortuosity of the extracellular and intracellular space, and increased intracellular viscosity are thought to contribute to the reduced mobility of free water (11). A temporal evolution of diffusion change occurs in ischemic brain tissue along with neuropathological events (13, 14). Acute ischemia can produce cytotoxic edema and thus, profound restriction in water diffusion in affected brain tissue within minutes after the onset of ischemia, when no signal changes are observed on T2 weighted images (15-18). The exclusion of patients who had an unexpected postoperative course represents a bias in this study; however we wanted to exclude the patients with acute hematoma and overt arterial acute occlusions during the early postoperative period because we did not aim to observe the diffusion changes in these situations, which were already examined in detail in previous reports (11, 19). Restricted diffusion patterns were more common in patients that had a supratentorial surgical approach. The supratentorial interventions were performed through cortical incisions and the removal of the lesions required both retraction and mechanical contact with the surrounding normal tissue. Any process that results in acute intracellular swelling and a subsequent decrease in the surrounding extracellular space can lead to restricted proton diffusion in the brain. After brain tumor resection, due to a variety of reasons, such as di-

rect surgical trauma, retraction and vascular injury, and devascularization of the tumor, acute cellular damage occurs (1, 2).

The appearance of hemorrhages on DWI has been the subject of several previous studies and was found to be influenced by many factors such as relative amounts of different hemorrhagic products and pulse sequences used (11). The oxygenation state of hemoglobin and lysis of initially intact red blood cell (RBC) membranes are 2 important factors that determine the MRI signal intensity patterns of hematomas. Shrinkage of extracellular space due to resorption of plasma with clot retraction (20), alterations of RBCs' shapes (21), a conformational change of the hemoglobin within RBCs (22), and contraction of intact RBCs (23) account for possible biophysical causes of restriction of diffusion in the early stages of hematomas. In early stage hematomas, RBCs are intact and contain relatively oxygenated hemoglobin (24). Oxyhemoglobin has been seen as hyperintense on DWI with lower ADC than normal brain tissue, suggesting reduced mobility of water protons inside the RBCs (19, 25). The T2-shine-through effect in hyperacute hematomas may be another contributor of the signal intensity on DWI, in contrast to hyperacute ischemic stroke, which lacks T2 signal intensity changes (26).

Hemorrhages coexist with ischemic changes very frequently during the early postoperative period. Given that there is a body of evidence that intracellular blood products produce high signals on DWI and low ADC values in first 3 stages of a hematoma (i.e., oxyhemoglobin, deoxyhemoglobin, and intracellular methemoglobin), hemorrhages may have been due to restricted diffusion in a number of patients in this series (26).

In our study, restricted diffusion was also the most common diffusion abnormality in cases accompanied by hemorrhages. As in most cases, MRIs were performed upon completion of each surgery and before transportation of the patients into the intensive care unit in this study; therefore, we can suggest that existing blood was in the oxy- deoxyhemoglobin state during the examination in most cases. To determine if high signals on DWI were due to blood or surgery-related tissue damage, GRE imaging and/or CTs were also obtained in this study (27). Echo-planar MRIs (EPI) with a b value of 0 s/mm^2, which have been found to be sensitive to detect hemorrhages nearly as effectively as GRE, were evaluated in order to determine the presence of hemorrhages around the surgery site in patients without GRE imaging or CT (28). Smith et al. widely described diffusion abnormalities in the early post-operative period and their long-term follow-up; however, they did not study hemorrhage-related changes in and around the resection cavity or their signal abnormalities on DWI. In early postoperative imaging, it is important to be aware of the misinterpretation of restricted diffusion due to a hemorrhage as tissue ischemia near the operation site.

In the present study, 7 patients (13.4%) showed increased diffusion and 4 patients had no signal abnormalities in the parenchyma neighboring the resection site on DWI. Increased diffusion might have been caused by both vasogenic edema and/or residual tumors in our cases. Altered blood-brain barrier permeability and subsequent extracellular space enlargement via water shift from the blood vessel may have been the cause of the observed increased diffusion. The presence of a residual tumor might also affect the signal intensity on DWI (5). Hodozuka et al. showed that local capillary permeability changes occurred more frequently in the postoperative period following tumor-resection than following normal brain tissue resection; however, we found no significant relationship between diffusion changes and tumor or non-tumor cases (29). Demarcation of a residual tumor from the surrounding vasogenic edema may be possible in some patients, but determining if there is a residual tumor by diffusion patterns without a comparative pre-operative DWI is not a reliable method.

Although the number of serial DWIs in this study was limited, in the cases with restricted diffusion, a return to baseline was observed on the repeat studies performed between the 7th postoperative day and one month. This pseudonormalization increases the likelihood that surgery-related changes, rather than tumor cell infiltration, was the cause of restricted diffusion.

Variable signal abnormalities may occur in the brain tissue near the operation site on early postoperative DWI. Restricted diffusion due to surgery-related acute changes and/or hyperacute blood was the most common DWI pattern in this series. Thus, in early postoperative imaging, radiologists should recognize whether restricted diffusion is due to hemorrhaging, as tissue damage may also occur near the operation site.

References

1. Cha S. Update on brain tumor imaging: from anatomy to physiology. AJNR Am J Neuroradiol 2006; 27: 475-487.
2. Smith JS, Cha S, Mayo MC et al. Serial diffusion-weighted magnetic resonance imaging in cases of glioma: distinguishing tumor recurrence from postresection injury. J Neurosurg 2005; 103: 428-438.
3. Bammer R. Basic principles of diffusion-weighted imaging. Eur J Radiol 2003; 45: 169-184.
4. Moritani T, Shrier DA, Numaguchi Y, et al. Diffusion-weighted echo-planar MR imaging: clinical applications and pitfalls. A pictorial essay. Clin Imaging 2000; 24:181-192.
5. Beauchamp NJ, Ulug AM, Passe TJ, et al. MR diffusion imaging in stroke: review and controversies. Radiographics 1998; 18:1269-1283.
6. Roley HA, Grant PE, Roberts TPL. Diffusion MR imaging. Theory and applications. Neuroimaging Clin North Am 1999; 9:343-361.
7. Ebisu T, Naruse S, Horikawa Y, et al. Discrimination between different types of white matter edema with diffusion-weighted MR imaging. J Magn Reson Imaging 1993; 3:863-868.
8. Ebisu T, Tanaka C, Umeda M, et al. Discrimination of brain abscess from necrotic or cystic tumors by diffusion-weighted echo-planar MR imaging. Magn Reson Imaging 1996; 14:1113-1116.
9. Tien RD, Felsberg GJ, Friedman H, et al. MR imaging of high-grade cerebral gliomas: value of diffusion-weighted echo-planar pulse sequence. AJR Am J Roentgenol 1993; 162: 671-677.
10. Ono J, Harada K, Mano T, et al. Differentiation of dys- and demyelination using diffusion anisotrophy. Pediatr Neurol 1997; 16:63-66.
11. Schaefer PW, Grant PE, Gonzalez RG. Diffusion-weighted MR Imaging of the Brain. Radiology 2000; 217:331-345.
12. Huisman TAG. Diffusion-weighted imaging: basic concepts and application in cerebral stroke and head trauma. Eur Radiol 2003; 13:2283-2297.
13. Warach S, Chien D, Li W, et al. Fast magnetic resonance diffusion-weighted imaging of acute human stroke. Neurology 1992; 42:1717-1723.
14. Schlaug G, Siewert B, Benfield A, et al. Time course of the apparent diffusion coefficient (ADC) abnormality in human stroke. Neurology 1997; 49:113-119
15. Chien D, Kwong KK, Gres DR, et al. MR diffusion-weighted imaging of cerebral infarction in humans. AJNR Am J Neuroradiol 1992; 13:1097-1102.

16. Mintorovitch J, Yang GY, Shimizu H, et al. Diffusion-weighted magnetic resonance imaging of acute focal cerebral ischemia: comparison of signal intensity with changes in brain water and Na+, K(+)- ATPase activity. J Cereb Blood Flow Metab 1994; 14:332-336.
17. Kucharczyk J, Vexler ZS, Roberts TP, et al. Echo-planar perfusion sensitive MR imaging of acute cerebral ischemia. Radiology 1993; 188:711-717.
18. Matsumoto K, Lo EH, Pierce AR, et al. Role of vasogenic edema and tissue cavitation in ischemic evolution on diffusion-weighted imaging: comparision with multiparameter MR and immunohistochemistry. AJNR Am J Neuroradiol 1995; 16:1107-1115.
19. Atlas SW, Dubois P, Singer MB, et al. Diffusion measurements in intracranial hematomas: implications for MR imaging of acute stroke. AJNR Am J Neuroradiol 2000; 29:1190-1194.
20. Latour L, Svoboda K, Mitra P, et al. Time-dependent diffusion of water in a biological model system. Proc Natl Acad Sci USA 1994; 91:1229-1233.
21. Hijiya N, Horuiuchi K, Asakura T. Morphology of sickle cells produced in solutions of varying osmolarities. J Lab Clin Med 1991; 117:60-66.
22. Kaibara M. Rheology of blood coagulation. Biorheology 1996; 33:101-117.
23. Hargens A, Bowie L, Lendt D, et al. Sickle-cell hemoglobin: fall in osmotic pressure upon deoxygenation. Proc Natl Acad Sci USA 1980; 77: 4310-4312.
24. Atlas S, Thulborn K. MR detection of hyperacute parenchymal hemorrhage of the brain. AJNR Am J Neurorad 1998; 19:1471-1507.
25. Kang BK, Na DG, Ryoo JW, et al. Diffusion-weighted MR imaging of intracerebral hemorrhage. Korean J Radiol 2001; 2:183-191.
26. Silvera S, Oppenheim C, Touze E, et al. Spontaneous intracerebral hematoma on diffusion-weighted images: influence of T2-shine-through and T2-blackout effects. AJNR Am J Neuroradiol 2005; 26:236-241.
27. Sohn CH, Baik SK, Lee HJ, et al. MR imaging of hyperacute subarachnoid and intraventricular hemorrhage at 3T: a preliminary report of gradient echo T2*-weighted sequences. AJNR Am J Neuroradiol 2005; 26:662-665.
28. Lu CY, Chiang IC, Lin WC, Kuo YT, Liu GC. Detection of intracranial hemorrhage: comparison between gradient-echo images and b0 images obtained from diffusion-weighted echo-planar sequences on 3.0 T MRI. Clin Imaging 2005; 29:155-161.
29. Hodozuka A, Sako K, Yonemasu Y. Sequential change of capillary permeability in the rat brain after surgical removal of an experimental brain tumor. J Neurooncol 1993; 16:191-200.